02,13

Superconducting thin films and tunnel junctions based on aluminum

© M.A. Tarasov[1], A.M. Chekushkin[1], M.Yu. Fominsky[1], D.M. Zaharov[2], A.A. Lomov[2], O.V. Devitsky[3,4], A.A. Gunbina[5], E.T. Sohina[6,7], V.S. Edelman[7]

[1] Kotelnikov Institute of Radio Engineering and Electronics, Russian Academy of Sciences, Moscow, Russia
[2] Valiev Institute of Physics and Technology, Russian Academy of Sciences, Moscow, Russia
[3] Southern Scientific Center, Russian Academy of Sciences, Rostov-on-Don, Russia
[4] North-Caucasian Federal University, Stavropol, Russia
[5] Institute of Applied Physics, Russian Academy of Sciences, Nizhny Novgorod, Russia
[6] NRU Higher School of Economics, Moscow, Russia
[7] Kapitza Institute for Physical Problems, Russian Academy of Sciences, Moscow, Russia

E-mail: tarasov@hitech.cplire.ru

Received April 29, 2022
Revised April 29, 2022
Accepted May 12, 2022

The features of conductivity in aluminum films produced by various methods are described depending on the presence of impurities, film thickness, and deposition conditions. The results of measuring the surface properties and crystal structure of fabricated films of aluminum, aluminum oxide, and aluminum nitride by X-ray diffraction and atomic force microscopy are presented. SIS, SIN, NIN junctions based on aluminum were fabricated using both shadow evaporation and magnetron sputtering. The current-voltage characteristics were measured. The prospects for improving the characteristics of aluminum SIS junctions, SQUID amplifiers, and SINIS detectors operating at temperatures of about 100 mK are discussed.

Keywords: aluminum thin films, surface roughness, atomically smooth films, tunnel junctions.

DOI: 10.21883/PSS.2022.10.54217.35HH

1. Introduction

Interest in quantum computers, qubits, bolometers and amplifiers with quantum sensitivity leads to a shift in priorities of modern superconducting electronics from high-temperature superconductivity to low-temperature one. Here, an essential role is played by superconducting aluminum, superconducting transmission lines, resonators and tunnel junctions based on it. In contrast to niobium, for aluminum, the presence of impurities and decrease in film thickness can lead not only to decrease in the critical current and critical temperature of nanosized objects (films and nanowires), but also to increase them. Aluminum is a classical type I superconductor. Doping with impurities and/or reducing the size of the sample can lead to such an object becoming a type II superconductor. The appearance of Abrikosov's vortices significantly changes the characteristics of both transmission lines and active elements such as SIS-, SIN-, and NIN-junctions. For tunnel junctions, in addition to the quasiparticle current, it is also necessary to take into account the Andreev current and leakage currents through vortex structures, the influence of the magnetic field, and overheating by the transport current.

Aluminum films used in practice have, as a rule, an amorphous or microcrystalline structure. For such films, the specific conductivity turns out to be lower than for films having a crystalline structure or for bulk samples. This is due to a decrease in the concentration of free electrons, the mean free path, an increase in the number of defects and boundaries between crystallites. Specific conductivity is a key parameter that determines losses in microwave structures.

2. Films and tunnel junctions

The deposition of aluminum films was performed by the methods of thermal evaporation from the boat heated by current, electron-beam evaporation from crucible, and magnetron sputtering. As an example, samples identical in size for measuring specific resistivity in the form of strips 0.2 mm wide and 10 mm long can be mentioned. At film thickness of 2 nm and less, the samples exhibited exceptionally high electrical resistance; the film, apparently, was of island type: and consisted of weakly bonded regions. At thickness of 6 nm, the specific resistivity was $\rho = 2 \cdot 10^{-6}\,\Omega \cdot \mathrm{m}$. For

films 20 nm thick $\rho = 2.9 \cdot 10^{-7}\,\Omega \cdot$ m. The resistance of films more than 300 nm thick approached the tabular value for bulk aluminum $\rho = 2.6 \cdot 10^{-8}\,\Omega \cdot$ m. At small thicknesses, the film consists of conductive islands separated by weakly conductive gaps, and as the thickness increases, the conductive regions merge. The low conductivity of amorphous thin films can be due to the localization of charge carriers on weakly bound clusters and the scattering of electrons by defects.

Samples of aluminum films of various thicknesses and impurity compositions were studied by atomic force microscopy and X-ray diffractometry. Typical AFM image of one of the aluminum films is shown in Fig. 1. The topographic image of the surface is characterized by rough relief and corresponds to a cluster structure with cluster sizes that correlate with the film thickness. On frequent occasions, macro-islands in the form of droplets up to several microns in size are observed on the surface of the films. As the film thickness increases to 30 nm, the size of the clusters increases almost linearly, and the lateral size exceeds the film thickness by one and half to two times. At thicknesses over than 50 and above than 100 nm, the growth of clusters practically stops.

For tunnel junctions, the height of the surface roughness profile from peak to trough (peak-to-peak) R_{pp}, which varies from 2 to 10 nm for film thickness from 3 to 130 nm for thermal evaporation [1], is of importance. Magnetron sputtering makes it possible to obtain smoother films with $R_{pp} = 5$ nm for a 150 nm film [2]. The conductivity and microwave properties depend on the lateral size of the crystallites, which are comparable to the film thickness during thermal deposition and up to 3 times larger in plan view during magnetron sputtering. The superconducting junction temperature of films 18 nm and 3 nm thick was 1.5 and 2.4 K. When aluminum was deposited at three oxygen pressure values of $(0-0.3-1) \cdot 10^{-5}$ mbar, the critical temperature was varied as 1.2–2.4–0 K and the sheet resistivity was varied as 20 nm film as 1.6 Ω–56 Ω–150 kΩ. As increase in the oxygen pressure, the increase in resistance of the film is observed with a simultaneous increase in the critical temperature to 2.4 K. Higher oxygen pressure leads to the transition of films to the dielectric state. In films evaporated with oxygen, significant surface distortions are observed in the form of dips and defects surrounded by aluminum ridges. These features correlate with the X-ray diffraction parameters of the films: the phase state, the texture of the crystal structure, and the size of the crystallites in the film.

Crystals of aluminum (cubic crystal, $Fm3m$) and its oxide (trigonal crystal, $R3\text{-}c$) belong to different crystal systems and have significantly different structure parameters: $a = b = c = 0.405$ nm, $\alpha = \beta = \gamma = 90°$ and $a = b = c = 0.518$ nm, $\alpha = \beta = \gamma = 29°$, respectively. Magnetron aluminum oxide films are in the X-ray amorphous phase; therefore, when aluminum films are deposited on aluminum oxide, growing crystallites predominantly have an arbitrary orientation. To elucidate the mechanisms of film

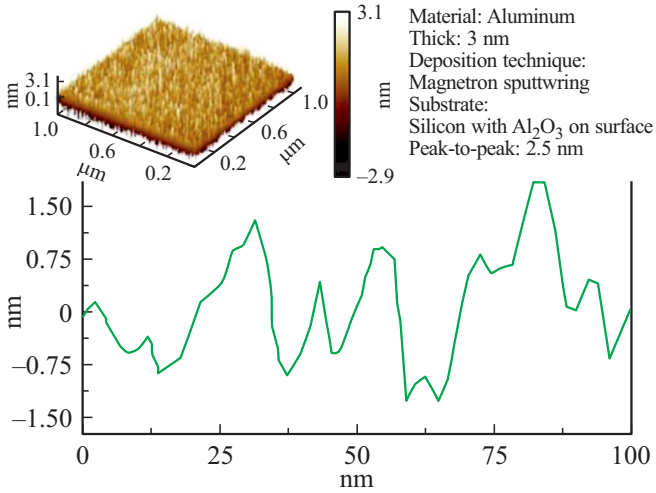

Figure 1. AFM image of the aluminum film 3 nm thick.

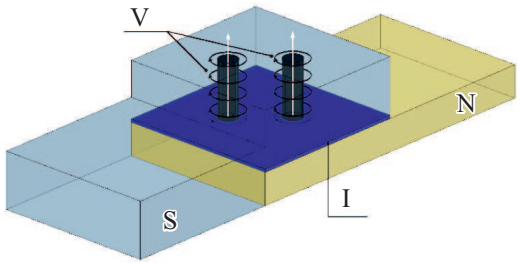

Figure 2. Schematic representation of the $1 \times 1\,\mu$m SIN-junction with two vortices $0.2\,\mu$m in diameter, where S is superconducting aluminum film, I is insulator, N is normal metal, V are vortices.

conductivity, we studied the magnetic field dependences of the volt-ampere characteristics of SIN-junctions based on them [3]. Pure crystalline aluminum is a type I superconductor with critical temperature 1.2 K, critical field 11 mT, a coherence length $1.5\,\mu$m, and London magnetic field penetration depth of 15–50 nm. The granular structure and impurities lead in our samples to increase in the critical temperature up to 2.4 K and the critical field up to 30 mT. The films begin to exhibit the properties of a type II superconductor with high upper critical field 28 mT, coherence length of 110 nm, and penetration depth of 300 nm. Even in a field of 4.6 mT, the conductivity of the SIN-junction at zero current bias becomes three orders of magnitude greater than without a field. In type II superconductor in magnetic field above the first critical field, Abrikosov's vortices penetrate in the film. For coherence length of 110 nm, the vortex area is $0.04\,\mu\text{m}^2$.

In this case, the conductivity at zero current bias increases by two orders of magnitude. Schematic representation of the SIN-junction with two Abrikosov's vortices is shown in Fig. 2. To fabricate tunnel junctions, the upper layer of aluminum was oxidized in oxygen atmosphere to obtain a specific resistivity of the order of 1 kΩ by $1\,\mu\text{m}^2$.

The properties of the barrier, its transparency, resistance, and current density should depend on the quality of the dielectric surface. In the case of atomically-smooth film, one can expect an increase in the current density, a decrease in the junction resistance, and a decrease in parasitic leakage associated with micro short-circuits. The influence of the magnetic field on the conductivity of junctions with films of various thicknesses is studied.

The results of the work show that magnetron-sputtered aluminum films thicker than 300 nm are optimal for preventing the appearance of vortices in SIS- and SIN-junctions. Further performance improvement can be achieved by using aluminum heteroepitaxial films, AlN and Al_2O_3 grown on a heated sapphire substrate [4]. To improve the electrical, thermal and microwave properties of structures based on aluminum films, series of studies of the technology of deposition of aluminum film of the first layer is being carried out, including long-term annealing of silicon (111) substrates in vacuum, deposition of a thin 5–8 nm seed layer without breaking the vacuum at temperature of 400°C, cooling to room temperature (and below), deposition of solid single-crystal film with a thickness of more than 300 nm. To form a tunnel barrier, the oxidation or nitridation of the atomically-smooth aluminum surface is performed. The crystal-lattice orientation of aluminum films is shown in Fig. 3. Then a second layer of aluminum with thickness of more than 300 nm is deposited. To form the area of tunnel junctions, the first electron-beam lithography is performed, followed by etching initially of the second aluminum layer, and then the first aluminum layer is etched according to the second electron lithography.

The detailed structure of the Al/Al_2O_3 interface remains slightly investigated. For the formation of tunnel junctions, it is important to elucidate the structure of the tunnel barrier,

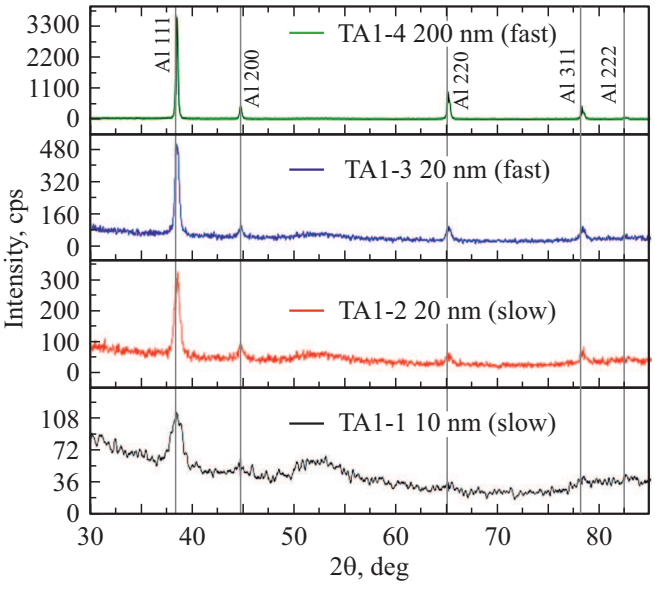

Figure 3. Structure of aluminum films 200, 20, 10 nm thick with fast and slow magnetron sputtering.

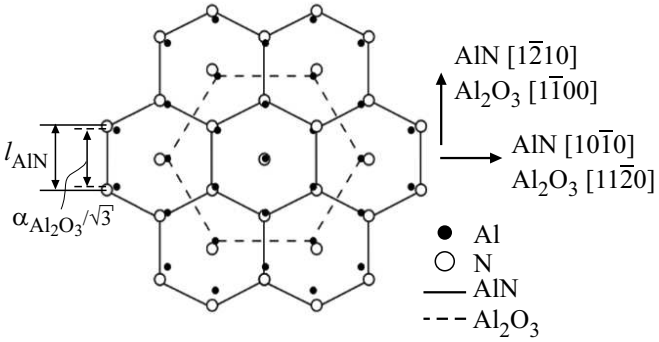

Figure 4. AlN film growth orientation diagram on *c*-plane of sapphire from [5].

which was the task of separate study. Thin AlN films were obtained on Al_2O_3 with the (0001) orientation using an ion-beam deposition setup, which included KLAN-53 ion source, growth station, and vacuum system. The residual gas pressure in the growth station was 10^{-4} Pa. Ion-beam deposition was carried out from aluminum target with purity of 99.99% in nitrogen-argon mixture atmosphere with used gases purity of 99.999%. The volume fraction of nitrogen in the nitrogen-argon mixture was 75%. The ion beam energy was 600 eV at the value of the ion current 40 mA. The deposition time was 60 min at a substrate temperature of 800°C. Annealing of the obtained samples was carried out in nitrogen atmosphere at pressure of 100 Pa, as well as in air in the temperature range of 800–950°C for 120 min. Note that the lattice parameters of such barriers differ noticeably from the tabulated ones, for AlN it is 0.31 nm, and for Al_2O_3 it is 0.47 nm. As an example, Fig. 4 shows diagrams of film growth on a sapphire substrate.

It can be seen from this figure that, with proper selection of material, substrate orientation, and deposition conditions, a smooth, defect-free barrier surface can be obtained.

3. Discussion

It should be noted that the fabrication of atomically-smooth silver films using a similar technology in [6] with a record low root-mean-square roughness RMS = 90 pm indicates the prospects for both scientific research and the development of industrial technology according to the patent [7].

The subnanometer geometric mean roughness should make it possible to increase the density of the superconducting critical current, as well as to reduce dielectric losses and fluctuations due to two-level tunnel systems. In quantum technologies, such properties are of decisive importance, since the quality factor and coherence are determined by the properties of superconducting tunnel junctions. Another important property of smooth barrier films is the high effective tunneling area. As we noted in [2], for rough films the area of the tunnel junction can be 10–20% of the sandwich area. If to divide the resistance quantum

value by the junction resistance, one can obtain the number of parallel conduction channels. Considering the diameter of such a channel to be equal to the coherence length, one can estimate the effective tunneling area. For our junctions of area $1\,\mu m^2$, the effective tunneling area can be 0.1, which is comparable to 0.13 in [8]. In this case, regions with a low tunneling current make almost the same contribution to the junction capacitance as the tunneling regions. This is because the tunneling current depends exponentially on the barrier thickness, while the capacitance depends linearly. As a result, in the case of atomically-smooth barrier, the effective tunneling area can approach the geometric area. This means a decrease in the specific capacitance of junctions by almost an order of magnitude. In the case of implementation for such a junctions, it is possible to significantly improve the electrodynamic characteristics and expand the spectral matching band.

On the other hand, even if assuming that the tunneling current density is the same over the entire area, then the area of the rough surface itself can be $1.5-2$ times larger than that of a smooth one, i.e. for a smooth surface, the area of the junction with the same resistance and current can be larger, which simplifies the requirements for the size of the junctions.

Funding

The work on the experimental study of the samples was carried out at Kotelnikov Institute of Radio Engineering and Electronics of RAS with the financial support of the RSF No. 21-42-04421. For the manufacture of samples, the equipment of Unique Scientific Facility #352529 „Cryointegral“ was used, the development of which was supported by a grant from the Ministry of Science and Higher Education of the Russian Federation, agreement No. 075-15-2021-667. X-ray diffraction experiments were performed at NUST „MISIS“ at the Department of Physical Materials Science using the equipment of the Center for X-Ray Diffraction Studies and Diagnostics of Materials. The work of A.A. Gunbina on the development of the topology for the samples was carried out at the IAP RAS with the support of the IAP RAS State Assignment No. 0030-2021-0005.

Conflict of interest

The authors declare that they have no conflict of interest.

References

[1] M.A. Tarasov, L.S. Kuzmin, N.S. Kaurova. Instrum. Exp. Tech. **52**, 877 (2009).
[2] M. Tarasov, A. Gunbina, M. Fominsky, A. Chekushkin, V. Vdovin, V. Koshelets, E. Sohina, A. Kalaboukhov, V. Edelman. Electronics **10**, 2894 (2021).
[3] M. Tarasov, V. Edelman. JETP Lett. **101**, 740 (2015).
[4] D.L. Medlin, K.F. McCarty, R.Q. Hwang. Thin Solid Films **299**, 110 (1997).
[5] M.G. Ambartsumov. Cand. dis. Vliyaniye usloviy plazmoaktivirovannogo atomnosloyevogo osazhdeniya na mikrostrukturu, sostav i svoystva plenok nitrida alyuminiya. (2020) (In Russian).
[6] I.A. Rodionov, A.S. Baburin, A.R. Gabidullin, S.S. Maklakov, S. Peters, I.A. Ryzhikov, A.A. Andriyash. Sci. Rep. **9**, 12232 (2019).
[7] I.A. Rodionov, A.S. Baburin, I.A. Ryzhikov. Single-crystalline metal films. Patent US 2021/00/0071292 A1/
[8] T. Greibe, M. Stenberg, C. Wilson, T. Bauch, V. Shumeiko, P. Delsing. Phys. Rev. Lett. **106**, 097001 (2011).

Editor K.V. Emtsev